

# Near field Exposure Assessment of Complex Anatomical Structures in 5G Bands

Giulia Sacco, Ante Lojic Kapetanovic, Dragan Poljak, Maxim Zhadobov

## ▶ To cite this version:

Giulia Sacco, Ante Lojic Kapetanovic, Dragan Poljak, Maxim Zhadobov. Near field Exposure Assessment of Complex Anatomical Structures in 5G Bands. 2023 XXXVth General Assembly and Scientific Symposium of the International Union of Radio Science (URSI GASS), Aug 2023, Sapporo, Japan. 10.23919/URSIGASS57860.2023.10265446 . hal-04248606

# HAL Id: hal-04248606 https://cnrs.hal.science/hal-04248606

Submitted on 18 Oct 2023

**HAL** is a multi-disciplinary open access archive for the deposit and dissemination of scientific research documents, whether they are published or not. The documents may come from teaching and research institutions in France or abroad, or from public or private research centers.

L'archive ouverte pluridisciplinaire **HAL**, est destinée au dépôt et à la diffusion de documents scientifiques de niveau recherche, publiés ou non, émanant des établissements d'enseignement et de recherche français ou étrangers, des laboratoires publics ou privés.



# Near field Exposure Assessment of Complex Anatomical Structures in 5G Bands

G. Sacco\*(1), A. Kapetanović(1), D. Poljak(2) and M. Zhadobov(1)

- (1) Institut dÉlectronique et des Technologies du numéRique (IETR), University of Rennes 1 CNRS, UMR 6164, F-35000 Rennes, France; e-mail: giulia.sacco@univ-rennes.fr; maxim.zhadobov@univ-rennes.fr
- (2) Faculty of Electrical Engineering, Mechanical Engineering and Naval Architecture (FESB), University of Split, 21000 Split, Croatia; e-mail: akapet00@gmail.com; dpoljak@fesb.hr

#### **Abstract**

With the proliferation of 5G wireless networks, the population is increasingly exposed to frequencies approaching the millimeter-wave (mmW) range. Human ears are among the most exposed body parts. This paper proposes an analysis of the ear exposure in the near field using an anatomical model in presence of different electromagnetic (EM) sources (vertical dipole, horizontal dipole,  $4 \times 4$  array of vertical dipoles, and  $4 \times 4$  array of horizontal dipoles). This study demonstrates that, for a given input power and antenna-ear distance, the absorbed power density ( $S_{ab}$ ) induced by a dipole antenna array is up to 3.9 times higher than the one produced by a single dipole.  $S_{ab}$  is only slightly sensitive to the dipole orientation (vertical or horizontal) resulting in relatively weak variations (up to 7%).

#### 1 Introduction

With the proliferation of 5G wireless networks, new frequency bands (including 24–28 GHz range) have been proposed to enable reduced latency and higher data rates. This will introduce to the environmental electromagnetic (EM) spectrum frequencies to which population has never been exposed so far.

For exposure assessment at millimeter-wave (mmW), due to a high computational cost and the shallow penetration depth (e.g., roughly 0.85 mm at 30 GHz), mainly monoor multi-layer planar tissue models have been used [1, 2]. However, some of the most exposed body parts cannot be accurately modelled as planar [3]. In [4], the authors compared the exposure of anatomical models of abdomen and wrist at 24 GHz with multi-layer tissue models. The findings demonstrated that the electric field distribution could not be accurately reproduced by a planar model. In [5], the exposure of forearm was investigated in the 6-60 GHz range. The EM energy absorption in the head and hand at 60 GHz was discussed in [6]. The exposure of body parts with smaller curvature radii, comparable to the wavelength in the mmW range, was performed in [3] with simplified cylindrical based models and in [7] for an anatomical ear model, considering a plane wave as source.

This paper aims at quantifying the power absorption in the human ear in the near field for different realistic antenna sources.

#### 2 Materials and Methods

#### 2.1 EM Model and Scenario

We considered a homogenous anatomical model of the adult ear with the typical dimensions and the complex permittivity of dry skin at 26 GHz (17.71 - j16.87) [8].

To evaluate the EM power deposition, we used 4 radiating sources: vertical dipole, horizontal dipole,  $4 \times 4$  array of vertical dipoles, and  $4 \times 4$  array of horizontal dipoles (Figure 1).

The input power was set to  $10\,\mathrm{mW}$ . The antenna sources are centred with respect to the ear model in the yz plane and the distance from the model surface (x direction) was varied from 5 mm to 15 mm with a 5 mm step. The model was simulated using COMSOL Multiphysics with the finite element method (FEM) technique. It was discretized with a tetrahedral mesh with a maximum cell size of  $\lambda/8$ . Perfectly matched layer (PML) was used as boundary condition.

### 2.2 Averaged Absorbed Power

Above 6 GHz, according to the international guidelines of International Commission on Non-ionizing Radiation Protection (ICNIRP) and International Electrical and Electronics Engineers (IEEE), the main dosimetric quantity is the absorbed power density [9, 10]

$$S_{ab} = \frac{1}{2A} \iint_A \Re \left[ E(y, z) \times H^*(y, z) \right] \hat{n} \, dA, \qquad (1)$$

where E and H are the peak values of the electric and magnetic fields on the model surface, respectively,  $\Re$  is the real part operator, \* is the complex conjugate operator, A is the averaging area, and  $\hat{n}$  dA is the integral variable vector,  $\hat{n}$  being the unit vector field normal to the surface.

 $S_{\rm ab}$  was evaluated over the entire ear surface to find the coordinates of the most exposed area (worst-case scenario).

This paper's copyright is held by the author(s). It is published in these proceedings and included in any archive such as IEEE Xplore under the license granted by the Agreement Granting URSI and IEICE Rights Related to Publication of Scholarly Work.

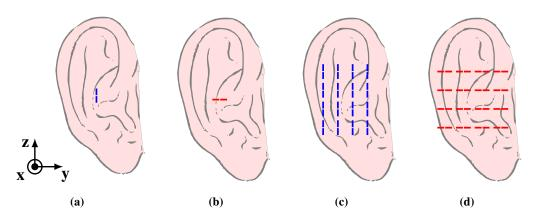


**Figure 1.** Exposure scenarii: (a) vertical dipole, (b) horizontal dipole, (c)  $4 \times 4$  array of vertical dipoles, and (d)  $4 \times 4$  array of horizontal dipoles.

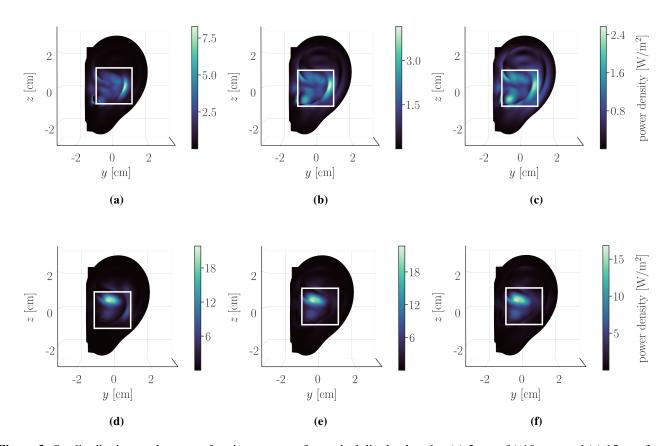


**Figure 2.**  $S_{ab}$  distribution on the ear surface in presence of a vertical dipole placed at (a) 5 mm, (b) 10 mm, and (c) 15 mm from the model surface and of a  $4 \times 4$  array of vertical dipoles placed at (d) 5 mm, (e) 10 mm, and (f) 15 mm from the model surface.

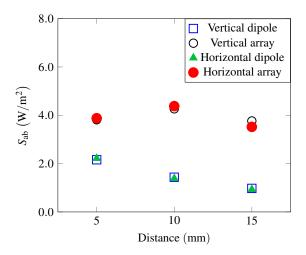


**Figure 3.**  $S_{ab}$  as a function of the distance.

The averaging area used to compute  $S_{ab}$  is the area conformal to the ear surface and limited by a  $2 \times 2$  cm square, that is typically larger than  $4 \text{ cm}^2$  due to the non planarity of the model [7].

#### 3 Results

The  $S_{ab}$  distribution over the ear surface for a vertical dipole and a  $4 \times 4$  array of vertical dipoles placed at 5 mm, 10 mm, and 15 mm from the model surface is reported in Figure 2. Similar distributions were obtained also for a horizontal dipole and dipole array (not shown in Figure 2). The white squares highlight the considered averaging area, which corresponds to the highest  $S_{ab}$  (worst-case). As it is possible to notice, the dipole array produces stronger  $S_{ab}$  values and the most exposed area is concentrated in a few millimetres region.

The results of  $S_{ab}$  averaged on the white squares as a function of the distance is shown in Figure 3. For a single dipole,  $S_{ab}$  decreases monotonically with the distance. However, when considering a  $4 \times 4$  array, regardless of the dipoles' orientation,  $S_{ab}$  is greater at the separation distance of 10 mm comparing to 5 mm. This may be explained by the different antenna-ear interactions occurring in the near field [11]. For a given distance, the difference in exposure between the two antenna orientations is limited to 4.7% and 7% for the single dipole and dipole array, respectively. For the same input power,  $S_{ab}$  is up to 3.9 times higher for the array than for the single dipole for vertical orientation and 3.8 times for horizontal orientation.

#### 4 Conclusion

This paper evaluates the near field exposure of the ear anatomical model at 26 GHz. A dipole and a  $4 \times 4$  array of dipoles with vertical and horizontal orientations were considered as EM sources.

For the same input power (10 mW) and distance, the array was responsible for higher values of  $S_{ab}$  (up to 4.4 W/m<sup>2</sup>) than the single dipole (up to 2.1 W/m<sup>2</sup>), while the difference in terms of antenna orientation (vertical or horizontal) had almost no impact on  $S_{ab}$  (up to 7% difference). The quantification of the resulting temperature rise is out of the scope of this paper, but constitutes one of its perspectives.

### Acknowledgements

This research was supported by the European Regional Development Fund under the grant KK.01.1.1.01.0009 (DAT-ACROSS), the French National Research Program for Environmental and Occupational Health of ANSES under Grant 2018/2 RF/07 through the NEAR 5G Project, and the European Unions Horizon Europe research and innovation program through the Marie Skłodowska-Curie IN-SIGHT project N°101063966.

#### References

- [1] K. Sasaki, M. Mizuno, K. Wake, and S. Watanabe, "Monte Carlo Simulations of Skin Exposure to Electromagnetic Field from 10 GHz to 1 THz," *Physics in Medicine & Biology*, vol. 62, no. 17, pp. 6993–7010, Aug. 2017.
- [2] A. Christ, T. Samaras, E. Neufeld, and N. Kuster, "RF-induced temperature increase in a stratified model of the skin for plane-wave exposure at 6-100 GHz," *Radiation Protection Dosimetry*, vol. 188, no. 3, pp. 350–360, Jun. 2020.
- [3] G. Sacco, Z. Haider, and M. Zhadobov, "Exposure levels induced in curved body parts at mmWaves," *IEEE Journal of Electromagnetics, RF and Microwaves in Medicine and Biology*, vol. 6, no. 3, pp. 413–419, Jun. 2022.
- [4] M. Colella, S. D. Meo, M. Liberti, M. Pasian, and F. Apollonio, "Numerical comparison of plane wave propagation inside realistic anatomical models and multilayer slabs," in 2022 52nd European Microwave Conference (EuMC). Milan: Institution of Engineering and Technology, Sep. 2022, pp. 800–803.
- [5] Y. Diao, E. A. Rashed, and A. Hirata, "Assessment of absorbed power density and temperature rise for nonplanar body model under electromagnetic exposure above 6 GHz," *Physics in Medicine & Biology*, vol. 65, no. 22, p. 224001, Nov. 2020.
- [6] A. R. Guraliuc, M. Zhadobov, R. Sauleau, L. Marnat, and L. Dussopt, "Near-field user exposure in forth-coming 5G scenarios in the 60 GHz band," *IEEE Transactions on Antennas and Propagation*, vol. 65, no. 12, pp. 6606–6615, Dec. 2017.
- [7] A. L. Kapetanovic, G. Sacco, D. Poljak, and M. Zhadobov, "Area-averaged transmitted and absorbed power density on a realistic ear model," *IEEE*

This paper's copyright is held by the author(s). It is published in these proceedings and included in any archive such as IEEE Xplore under the license granted by the Agreement Granting URSI and IEICE Rights Related to Publication of Scholarly Work.

- Journal of Electromagnetics, RF and Microwaves in Medicine and Biology, 2022.
- [8] C. Gabriel, "Compilation of the dielectric properties of body tissues at RF and microwave frequencies." Defense Technical Information Center, Fort Belvoir, VA, Tech. Rep., Jan. 1996.
- [9] International Commission on Non-Ionizing Radiation Protection (ICNIRP), "Guidelines for limiting exposure to electromagnetic fields (100 kHz to 300 GHz)," *Health Physics*, vol. 118, no. 5, pp. 483–524, May 2020
- [10] International Electrical and Electronics Engineers (IEEE), "IEEE standard for safety levels with respect to human exposure to electric, magnetic, and electromagnetic fields, 0 Hz to 300 GHz," 2019.
- [11] M. Ziane, R. Sauleau, and M. Zhadobov, "Antenna/body coupling in the near-field at 60 GHz: Impact on the absorbed power density," *Applied Sciences*, vol. 10, no. 21, p. 7392, Oct. 2020.